# Tunable phase-shifted fiber Bragg grating based on femtosecond laser fabricated in-grating bubble

**Changrui Liao,[1,3] Lei Xu,[2] Chao Wang,[3] D. N. Wang,[3] Yiping Wang,[1,]\* Qiao Wang,[1] Kaiming Yang,[1] Zhengyong Li,[1] Xiaoyong Zhong,[1] Jiangtao Zhou,[1] and Yingjie Liu[1]**

[1]*Key Laboratory of Optoelectronic Devices and Systems of Ministry of Education/Guangdong Province, Shenzhen University, Shenzhen 518060, China*

[2]*School of Software Engineering, Shenzhen Institute of Information Technology, Shenzhen, Guangdong 518029, China*

[3]*Department of Electrical Engineering, The Hong Kong Polytechnic University, Hung Hom, Kowloon, Hong Kong, China*
*\*Corresponding author: ypwang@szu.edu.cn*

We present a type of phase-shifted fiber Bragg gratings based on an in-grating bubble fabricated by femtosecond (fs) laser ablation together with a fusion-splicing technique. A microchannel vertically crossing the bubble is drilled by fs laser to allow liquid to flow in or out. By filling different refractive index (RI) liquid into the bubble, the phase-shift peak is found to experience a linear red shift with the increase of RI, while little contribution to the change of phase shift comes from the temperature and axial strain. Therefore, such a PS-FBG could be used to develop a promising tunable optical filter and sensor.   © 2013 Optical Society of America

*OCIS codes:*  (060.2370) Fiber optics sensors; (060.3735) Fiber Bragg gratings; (140.7090) Ultrafast lasers.
http://dx.doi.org/10.1364/OL.38.004473

As one type of the most successful bandpass filters, phase-shifted fiber Bragg grating (PS-FBG) has a wide range of applications in distributed feedback (DFB) lasers [1], switching elements in dense wavelength-division-multiplexing (DWDM) optical communication systems [2], and sensors for strain and liquid refractive index (RI) [3–6].

Many techniques have been reported for PS-FBG fabrication. The commonly used one is to employ a phase-shifted phase mask in the single exposure process [7]. Such a method possesses good repeatability but poor flexibility because the grating wavelength is determined by the period of the phase mask, and various phase masks are required for different grating wavelengths. In the transverse holographic double exposure process (Moiré method) method [8], two spatially colocated FBGs with slightly different Bragg wavelengths are inscribed in a sequential exposure process, achieved by tuning the laser wavelength, shifting the fiber that is perpendicular to the fiber axis, or applying strain to the fiber before inscribing the second FBG. The Moiré method requires a precise control to guarantee the correct phase shift and hence is of high cost. An alternative is to use the moving fiber-scanning beam approach in which the fiber is mounted on a personal computer (PC)-controlled PZT stage that can be slowly moved relative to the phase mask, allowing a phase shift to be incorporated into the grating [9]. The difficulty existing in the method is to accurately control the relative shift between the fiber and the phase mask. Postprocessing techniques using ultraviolet (UV) laser [10] or $CO_2$ laser [11] have also been reported for PS-FBG fabrication. By use of focused laser beam to illuminate the fiber grating region, a local RI is induced, thus creating a phase shift in the grating. However, UV postprocessing requires extra exposed time (typically up to hours) while $CO_2$ laser postprocessing may be difficult to implement for short FBGs due to its large spot size. Although PS-FBG can also be fabricated by external perturbations techniques such

as applying heating [12,13] or local pressure [14], the temporary phase shift will be removed from the grating in the absence of external disturbance.

In this Letter, we proposed a new technique to fabricate tunable PS-FBG by combining femtosecond (fs) laser micromachining together with fusion splicing. In such a device, the phase shift is introduced by an in-grating bubble, which is fabricated by three steps. First, drilling a microhole at the end facet of the fiber with part of FBG and then followed by fusion splicing with another fiber tip with the remaining FBG to form an in-fiber hollow sphere. Finally, a microchannel is inscribed by fs laser to vertically cross the hollow sphere to allow liquid to flow in or out. The response of the device to RI, temperature, and axial strain has been experimentally investigated. With the increase of ambient temperature or axial strain, the transmission spectrum of the device experiences a linear red shift; however, there is little change in the value of the phase shift. The phase-shifted peak of the grating can be tuned by filling different RI liquids inside the bubble and a RI sensitivity of ∼9.9 nm/RIU (refractive index unit) can be obtained. Such a device could be used to develop an ultracompact tunable bandpass filter by changing the RI liquid inside the bubble. By filling some functional liquids into the in-grating bubble such as liquid crystal, magnetic liquid, and biological reagent, such a device may find more applications in electro-controlled optical filter and various types of sensors.

Figure 1(a) shows the schematic diagram of the designed PS-FBG, which consists of a through bubble positioned on the center of the FBG. The fabrication procedure involved three steps: first, a 5 mm long FBG with a resonance wavelength of 1578 nm was written in SMF (Corning SMF-28e) by means of 193 nm ArF laser irradiation through a phase mask. Figure 2(a) shows the spectral properties of the obtained FBG, and there is a large transmission loss of ∼20 dB at the Bragg resonance wavelength and a negligible insertion loss. Second, the FBG was cut into two sections at the middle of the

grating using fiber cleaver. Then, one microhole with a diameter of ~3 μm was drilled at the center of the cleaved fiber-end facet by use of a Ti: sapphire fs laser system. In the fabrication process, the fs laser pulses ($\lambda = 800$ nm) with the duration of 120 fs and the repetition rate of 1 kHz were focused onto the fiber-end facet by a 20× objective lens with a NA value of 0.5 and a working distance of 2 mm. The group-velocity dispersion of the optical system was minimized by adjusting the amplifier of the laser system. The pulse energy was adjustable by rotating the half-wave plate incorporated with the polarizer and the on-target laser power was maintained at ~1 mW with irradiation time of ~1 s. The fiber tip with the microhole was spliced together with the other tip containing the rest of the FBG section by use of a fusion splicer (Ericsson FSU-975) with a fusing current of 16.3 mA and a fusing duration of 2.0 s. Since air in the microhole was suddenly heated, it rapidly expanded to a large hollow sphere with a smooth inner surface. The sphere diameter is measured to be ~50 μm. Third, a pair of microchannels was successively fabricated by fs laser drilling from both upper and lower fiber surface vertically to the bubble center to allow external liquid to flow in or out. Details of this fabrication process have been introduced in our previous paper [15,16]. The optical microscope image of the obtained PS-FBG is displayed in Fig. 1(b).

Figure 2(b) shows the spectra of the obtained PS-FBG in air. It can be seen from Fig. 2(b) that the micromachined in-grating microstructure induced an overall insertion loss of ~3.5 dB and a sharp phase-shift peak around the center of FBG stop band at 1578.8 nm with FWHM of 30 pm. While the bandwidth of the transmission stop band of the FBG is

~188 pm, it gives a finesse of 6.3 for this device. The finesse is comparable to that of PS-FBGs, fabricated by Moiré method [8] and can be further enhanced by raising the reflectivity of the FBGs.

Theoretically, the wavelength of the phase-shift peak depends on location and value of the introduced phase shift. In our configuration, the phase shift is introduced by producing a hollow sphere positioned at the RI modulation region of the grating. The amount of the phase shift depends on both the size of the bubble and the RI liquid inside the bubble. In light of this, the phase-shift peak can be easily adjusted by changing the RI liquid inside the bubble. In the experiment, the fabricated PS-FBG was immersed in series into different RI liquids (Cargille Laboratories, Inc.) to measure its response. After each measurement, the device was rinsed with propyl alcohol carefully until the original spectrum in air was restored so that no residual liquid was left. The transmission spectra were monitored in real time with an optical spectrum analyzer (OSA) with a resolution of 0.01 nm. Figure 3(a) shows the transmission spectra of the device in different RI liquids of 1.412, 1.414, 1.418, and 1.422, respectively. It can be clearly seen from Figs. 3(a) and 2(b) that as the RI liquid is inside the bubble, the transmission loss decreases by ~3.3 dB. The reason of this is that the reflectivity of the bubble inner surface is reduced due to the infiltration of the high RI liquid into the cavity. With the increase of RI, the phase-shift peak exhibits an obvious red shift and if the induced phase change exceeds $2\pi$, a new peak will be regenerated from the shorter wavelength side, as shown in Fig. 3(b), where a new cycle occurs when the RI changes from 1.408 to 1.412. The strength of the phase-shift peak also changes during
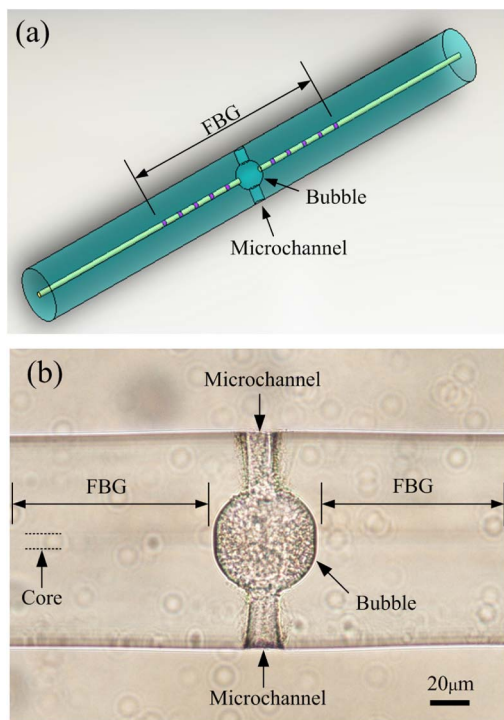


Fig. 1.   (a) Schematic diagram of the designed PS-FBG in single mode fiber. (b) Optical microscope image of the PS-FBG fabricated by fs laser ablation together with fusion splicing technique.
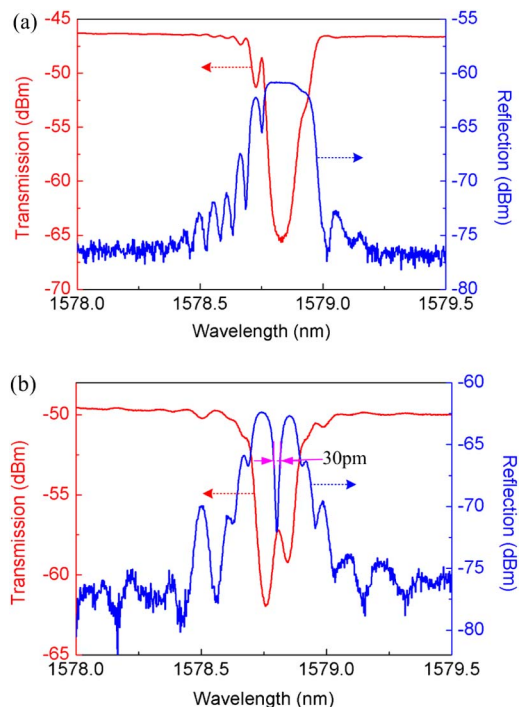


Fig. 2.   (a) Transmission (red line) and reflection (blue line) spectra of the FBG fabricated by 193 nm ArF laser through a phase mask. (b) Transmission (red line) and reflection (blue line) spectra of the fabricated PS-FBG.
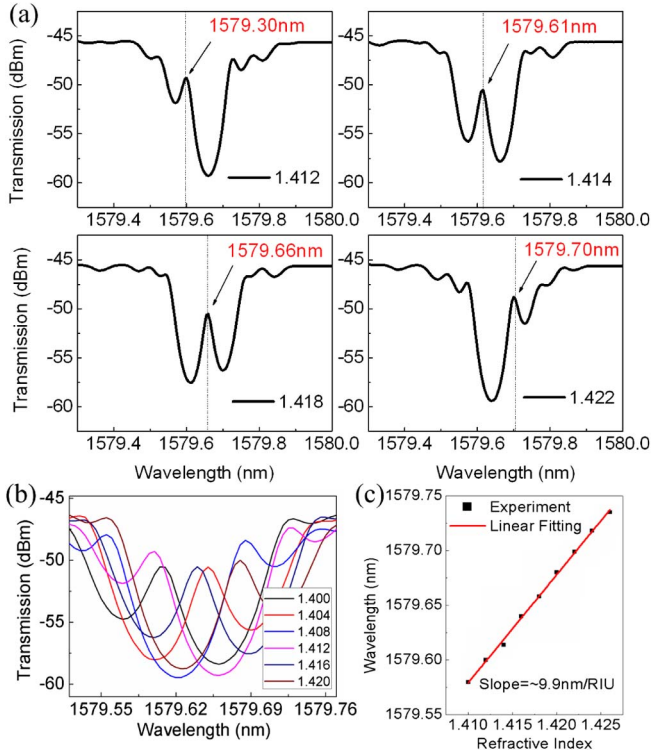
Fig. 3. (a) Spectral evolution of the microchannel PS-FBG subject to different RI liquids. (b) Cyclic feature of the PS-FBG filled by different RI liquids. (c) Linear relationship between the wavelength of the phase-shift peak and RI of the liquid, with a slope of ~9.9 nm/RIU.
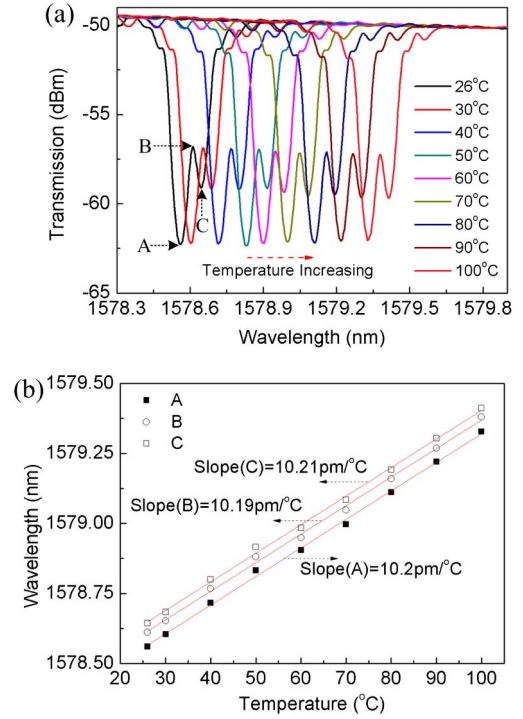


Fig. 4. (a) Transmission spectra the micromachined PS-FBG at different temperatures. (b) Linear relationship between the wavelength of extreme point of the transmission spectrum and the ambient temperature.

its shifting process and the peak becomes the strongest when it approaches to the center of the Bragg reflection band. Figure 3(c) shows the linear relationship between the phase-shift peak wavelength and the RI, where an RI sensitivity of ~9.9 nm/RIU is obtained.

The influence of temperature on the PS-FBG has been investigated by placing the device into an electrical oven and gradually increasing the temperature from room temperature to 100°C. Figure 4(a) shows the transmission spectra of the PF-FBG at different temperatures, and a red shift is clearly observed when the temperature is increased. The wavelengths at three extreme points in the transmission spectrum, i.e., A, B and C, were tracked and their relation with temperature are given in Fig. 4(b), where a linear relation is found, with temperature coefficients of ~10.21 pm/°C for "C," ~10.19 pm/°C for "B," and ~10.20 pm/°C for "A." That is to say, the rise of temperature hardly changes the amount of the introduced phase shift since the thermal expansion effect of the hollow sphere is negligible. The spectral temperature sensitivity of the PS-FBG is close to that of the uniform FBG, which is mainly resulting from the effective RI change of core mode by heating the fiber.

The effect of strain variation on the PS-FBG has also been investigated by stretching it along the fiber axis. Figure 5(a) shows the spectral evolution of the device with the increase of strain from 0 to 1000 με by a step of 100 με. It can be seen from this figure that the whole spectrum experiences a red shift with the increase of strain. Figure 5(b) shows the wavelengths at three extreme points when different strains were applied, and

a linear relation can be found, with strain coefficients of ~0.481 pm/με for "C," ~0.480 pm/με for "B," and ~0.485 pm/με for "A." The small difference of the strain coefficient among three extreme points means that the phase shift of grating is hardly changed by strain, similar to that induced by temperature. We believe the strain-induced spectral movement is mainly due to the elasto-optical effect of silica fiber.

However, compared with the uniform FBG without a phase shift (with a strain sensitivity of ~1.2 pm/με at ~1550 nm [17,18]), the PS-FBG demonstrates a much lower strain coefficient. This can be explained by the fact that when a stress is applied to the entire fiber, there will be an unequal load of strain along each section of the fiber, depending on the local mechanical resistance [19]. The stress loads applied to the bubble section and to the grating section are equal:

$$\varepsilon_B E A_B = \varepsilon_G E A_G, \tag{1}$$

represent the applied strains on the bubble and the grating section, and $A_B$ and $A_G$ refer to the cross-sectional areas of silica part within the bubble and the grating sections, respectively. Thus, the strains applied to these two regions just depend on the ratio of cross-sectional areas, $\varepsilon_G / \varepsilon_B = A_B / A_G$, and $A_B < A_G$. This means the fiber section with bubble bears more strain loads than the grating section; hence the strain sensitivity of the PS-FBG is depressed to some extent.

We found the spectral envelope of the PS-FBG remains unchanged in the RI test but exhibits a linear red shift with the increase of temperature or axial strain. Thus,
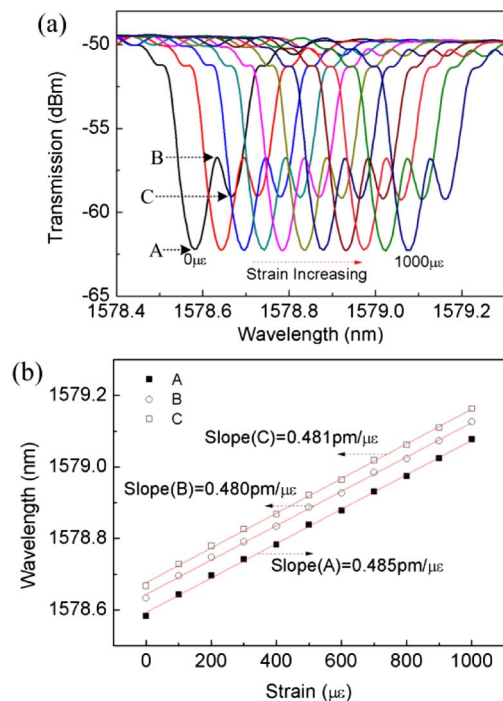
Fig. 5.   (a) Spectral evolution of the micromachined PS-FBG subject to different axial strains. (b) Linear relationship between the wavelengths of three extreme points of the transmission spectrum and the applied axial strain.

it is possible to eliminate the cross sensitivity of temperature and axial strain by measuring the envelope movement, and the location of the envelope can be set by the central wavelength of FWHM of the envelope.

In this Letter, we have experimentally demonstrated a tunable PS-FBG based on an in-grating bubble incorporated with a through microchannel. The in-grating bubble is fabricated using fs laser ablation assisted by fusion splicing method in a fiber with FBG. The microchannel is drilled by fs laser to allow liquid to flow in or out. The RI response of this PS-FBG has been investigated and the phase-shift peak shows a linear RI response with a sensitivity of ~9.9 nm/RIU, while the spectral envelope of the FBG remaining unchanged. Based on this property, the phase-shift value of the grating can be easily tuned by changing the RI liquid inside the bubble. With the increase of temperature or axial strain, the spectral envelope of the PS-FBG experiences a red shift with a temperature sensitivity of ~10.2 pm/°C or a strain sensitivity of ~0.48 pm/με, while the phase-shift value is hardly changed. Overall, the revealed linear RI response with little cross-sensitivity from temperature and axial strain of the in-grating-bubble PS-FBGs are of great advantage over conventional configurations. The device may find new applications in electro-controlled optical filter and various types of sensors, when filling into the bubble with functional liquid such as liquid crystal, magnetic liquid or biological reagent.

## References

1. J. T. Kringlebotn, J. L. Archambault, L. Reekie, and D. N. Payne, Opt. Lett. **19**, 2101 (1994).
2. X. H. Zou, M. Li, W. Pan, L. S. Yan, J. Azana, and J. P. Yao, Opt. Lett. **38**, 3096 (2013).
3. D. Gatti, G. Galzerano, D. Janner, S. Longhi, and P. Laporta, Opt. Express **16**, 1945 (2008).
4. K. M. Zhou, Z. J. Yan, L. Zhang, and I. Bennion, Opt. Express **19**, 11769 (2011).
5. Y. P. Wang, H. Bartelta, W. Ecke, R. Willsch, J. Kobelke, M. Kautz, S. Brueckner, and M. Rothhardt, Opt. Commun. **282**, 1129 (2009).
6. Y. J. Rao, X. Zeng, Y. Zhu, Y. P. Wang, T. Zhu, Z. L. Ran, L. Zhang, and I. Bennion, Chin. Phys. Lett. **18**, 643 (2001).
7. R. Kashyap, P. F. Mckee, and D. Armes, Electron. Lett. **30**, 1977 (1994).
8. L. Zhao, L. Li, A. Luo, J. Z. Xia, R. H. Qu, and Z. Fang, Optik **113**, 464 (2002).
9. W. H. Loh and R. I. Laming, Electron. Lett. **31**, 1440 (1995).
10. J. Canning and M. G. Sceats, Electron. Lett. **30**, 1344 (1994).
11. L. Xia, P. Shum, and C. Lu, Opt. Express **13**, 5878 (2005).
12. S. Gupta, T. Mizunami, and T. Shimomura, J. Lightwave Technol. **15**, 1925 (1997).
13. C. R. Liao, Y. H. Li, D. N. Wang, T. Sun, and K. T. V. Grattan, IEEE Sens. J. **10**, 1675 (2010).
14. C. J. S. Matos, P. Torres, L. C. G. Valente, W. Margulis, and R. Stubbe, J. Lightwave Technol. **19**, 1206 (2001).
15. C. R. Liao, T. Y. Hu, and D. N. Wang, Opt. Express **20**, 22813 (2012).
16. C. R. Liao, D. N. Wang, and Y. Wang, Opt. Lett. **38**, 757 (2013).
17. Y. J. Rao, Y. P. Wang, Z. L. Ran, T. Zhu, and B. M. Yu, Proc. SPIE **4581**, 327 (2001).
18. Y. P. Wang, H. Bartelt, M. Becker, S. Brueckner, J. Bergmann, J. Kobelke, and M. Rothhardt, Appl. Opt. **48**, 1963 (2009).
19. O. Frazão, S. F. O. Silva, A. Guerreiro, J. L. Santos, L. A. Ferreira, and F. M. Araújo, Appl. Opt. **46**, 8578 (2007).